



Total cancer risk estimates from measured concentrations of volatile organic compounds in industrialized southeastern Louisiana

Ellis S. Robinson^{a,1,2}, Amira Yassine^a, Shivang Agarwal^a, Mina W. Tehrani^{a,3}, Sara N. Lupolt^{a,b}, Andrea A. Chiger^{a,b,4}, Carolyn Gigot^{a,b,5}, Megan S. Clafin^c, Brian M. Lerner^c, Tara I. Yacovitch^d, Joseph R. Roscioli^d, Scott C. Herndon^d, Anita M. Avery^e, Conner Daube^d, Elizabeth M. Lunney^d, Edward C. Fortner^e, Benjamin S. Werden^{e,6}, Thomas A. Burke^a, Ana M. Rule^a, Kirsten Koehler^a, Keeve E. Nachman^{a,b}, and Peter F. DeCarlo^{a,1}

Affiliations are included on p. 10.

Edited by Julian D. Marshall, University of Washington, Seattle, WA; received March 10, 2025; accepted August 22, 2025, by Editorial Board Member Akkihebbal R. Ravishankara

Communities in southeastern Louisiana are subject to disproportionate environmental health burdens, including elevated risk for cancer, from emissions of industrial hazardous air pollutants (HAPs). However, there are few ambient measurements (or none) of various HAPs in the heavily industrialized corridor between Baton Rouge and New Orleans (BR-NO). We measured 17 carcinogenic volatile organic compounds using fast-response in situ instrumentation aboard a mobile laboratory. Using spatially resolved concentrations, we estimate cancer risk in 15 census tracts along an 81 km-long stretch of the BR-NO corridor. In 14 of 15 tracts, our estimates of total cancer risk were higher (range: 0.9 to 11.6×; median: 5×) than those from the U.S. Environmental Protection Agency's (USEPA) 2020 Air Toxics Screening Assessment (AirToxScreen). Our maximum estimate for total tract-level cancer risk was 560-in-one million excess cancer cases, far exceeding the upper limit of USEPA's acceptable risk range (100-in-one million). This discrepancy is largely explained by differences between measured vs. modeled ethylene oxide concentrations, though there are important contributions from a number of additional HAPs. Our risk estimates are dominated by ethylene oxide, which contributes between 39.5 and 92.2% of total cancer risk across all tracts; chloroprene (0.2 to 36.8%); and formaldehyde (4.1 to 14.6%). AirToxScreen also identifies these three compounds as primary drivers of risk in this location. Together, these three compounds account for between 63 and 96.9% of total cancer risk. There is substantial spatial variability in total cancer risk and the relative contribution of each HAP, both between and within tracts. These data substantiate claims that the region has high HAPs-related cancer risk and quantify which individual HAPs are of highest concern.

hazardous air pollutants | environmental justice | volatile organic compounds | cancer risk | mobile monitoring

Louisiana is a major hub for petrochemical industrial activity; it is home to roughly one-sixth of nationwide petroleum refining capacity (1) and is the second-largest chemicals exporting state in the United States (2). This activity is associated with large amounts of hazardous air pollutant (HAP) emissions, which are highly concentrated along the Mississippi River corridor between Baton Rouge and New Orleans (BR-NO). The BR-NO corridor comprises only 12% of the land area of the state, but contains 45% of the industrial facilities that report air releases in the United States Environmental Protection Agency's (USEPA) Toxic Releases Inventory (TRI) and 57% of mass emissions from TRI [year 2021 (3)].

Communities near these industries have raised concerns about their exposures to environmental pollutants, particularly volatile organic compound (VOC) air pollution (4–6). Recent research aims to quantify the adverse health impacts of this pollution (7, 8), and the inequality in exposures experienced by different populations in the BR-NO corridor (9–11). In 2022, USEPA investigated whether Louisiana's Department of Environmental Quality (LDEQ) and Department of Health (LDH) were responsible for discriminatory industrial permitting practices that put Black communities at increased cancer risk (12). Terrell and St. Julien (13) argue that permitting of industrial sites by the State of Louisiana has been racially discriminatory. The region has carried the nickname "Cancer Alley" since the 1980s, given to it by environmental activists in response to these concerns (14).

Significance

Southeastern Louisiana is home to many industrial point sources that emit toxic air pollutants. Residents do not have an accurate quantitative assessment of their related cancer risk due to a lack of data. We measured pollutants aboard a mobile laboratory to estimate excess cancer risk facing area residents and found "unacceptable" levels in all census tracts. Ethylene oxide dominated total cancer risk, with significant contributions from chloroprene and formaldehyde. There is an urgent need for comprehensive measurements of key carcinogenic air pollutants, especially in areas with a history of disproportionate environmental health burdens.

PNAS policy is to publish maps as provided by the authors.

¹To whom correspondence may be addressed. Email: esrobinson@arizona.edu or pdecarlo1@jhu.edu.

²Present address: Department of Chemical and Environmental Engineering, University of Arizona, Tucson, AZ 85721.

³Present address: Minnesota Pollution Control Agency, St. Paul, MN 55155.

⁴Present address: Department of Environmental Health Sciences, School of Public Health, Columbia University, New York City, NY 10032.

⁵Present address: ICF International, Inc., Reston, VA 20190.

⁶Present address: Department of Environmental Health and Engineering, Johns Hopkins University, Baltimore, MD 21205.

This article contains supporting information online at <https://www.pnas.org/lookup/suppl/doi:10.1073/pnas.2504770122/-DCSupplemental>.

Published October 6, 2025.

Most of the above studies (9, 10) rely on USEPA's Air Toxics Screening Assessment ["AirToxScreen," formerly National Air Toxics Assessment (NATA)] to understand and quantify inhalation exposures to HAPs (15), due to a lack of monitoring in the region. AirToxScreen provides model estimates of the ambient concentrations of HAPs using a hybrid approach that blends dispersion and chemical transport modeling (16). AirToxScreen relies on the National Emissions Inventory [NEI (17)], which often includes industry-reported emission values for HAPs from industrial point sources (18). For large swaths of the country where there is limited ambient monitoring of HAPs, which includes much of the BR-NO corridor, AirToxScreen can be the only available tool for quantifying exposures and health risks to HAPs.

There have been previous efforts to quantify the performance of AirToxScreen and NATA using ambient HAPs measurements. Most of these studies focus on specific geographies (e.g., individual urban areas or states) with the scope of the comparisons limited by the number of chemical species measured (19–24). While the results and conclusions vary across these studies, and even within a given study depending on the HAP, most conclude that the screening model underpredicts concentrations for a majority of HAPs. A few efforts have been made to compare AirToxScreen and NATA estimates systematically across the entire US. For example, Xue et al. (25) found that 2011 NATA concentration estimates for some chemicals (e.g., vinyl chloride, 1,1,2-trichloroethane) agreed with measurements within a factor of 2 across all sites from the 10 EPA regions, while concentration estimates for other chemicals were widely overpredicted (e.g., formaldehyde) or underpredicted (e.g., chloroform, methyl chloride). Padilla et al. (26), using more-recent AirToxScreen estimates, showed systematically higher measured HAPs concentrations compared to AirToxScreen for a large majority of HAPs, including for chloroprene, ethylene oxide, and formaldehyde. Whether model-measurement concentration disagreements are important for cancer risk estimates depends on the product of the chemical species' ambient concentration and its cancer potency. A HAP's cancer potency is quantified by its inhalation unit risk (IUR) value; specifically, IURs can be used to estimate the increased cancer risk per $1 \mu\text{g m}^{-3}$ increase in air concentration of that HAP over a lifetime of exposure.

LDEQ does operate several monitoring stations in the region that regularly measure VOC HAPs (27); the measured compounds are a subset ($n = 59$ total, $n = 16$ carcinogens) of those VOC HAPs listed in Title III of the Clean Air Act Amendments of 1990 ($n = 97$; ref. 28). Importantly, however, some notable HAPs emitted in the region that have high cancer toxicity are not included in this analyte list, including ethylene oxide (IUR = $3 \times 10^{-3} \mu\text{g m}^{-3}$), chloroprene (IUR = $3 \times 10^{-4} \mu\text{g m}^{-3}$), and formaldehyde (IUR = $1.3 \times 10^{-5} \mu\text{g m}^{-3}$) (29–31). These monitoring sites quantify pollutant concentrations with intermittent (one-in-six day), long-average (24-h) sampling, which will not capture many intermittent plumes. Even if a comprehensive list of HAPs were measured, the spatial paucity of the monitoring network amid such a high density of industrial point sources makes it challenging to accurately assess exposures and cancer risk for communities located near facilities but far from a monitoring station. A region dense with large point sources of many different primary pollutants will have large spatial pollutant gradients that a sparse monitoring network is unable to represent. Many of the VOC HAPs emitted in the region are primary pollutants (meaning directly emitted, and typically without any secondary production), though some (notably

formaldehyde) can be formed through secondary atmospheric reactions. Measuring those HAPs present in the region with high toxicities, and at high spatiotemporal resolution, is thus required for accurately assessing exposures and potential health risks.

Mobile monitoring has emerged in recent years as an important tool for establishing how surface concentrations of air pollutants vary at high spatial resolution (32, 33). While air pollutant measurements from mobile platforms have a long history (e.g., aircraft measurement campaigns), it is only in recent decades that the technique has been applied to resolve concentrations representative of long-term averages at high spatial resolution. For instance, Apte et al., showed that long-term average concentrations at a given location can be derived from repeated visitations (≈ 10 to 15 visits) of a mobile laboratory using fast (~ 1 Hz) instrumentation (34) and appropriate spatiotemporal data aggregation. This technique has predominantly been applied to measuring the spatial variability of particulate matter (34), nitrogen dioxide (35), and other traffic-related pollutants in urban areas (36), though there are notable recent examples of using mobile monitoring to study air toxics (37–39).

Using a mobile laboratory and applying best-practice techniques to minimize spatiotemporal sampling bias, we quantified ambient concentrations for a large suite ($n = 17$) of carcinogenic VOC HAPs using advanced, real-time analytical instrumentation, some of which have not been previously measured in the region. The measurements were made during February 2023 as part of the HAP Monitoring and Assessment Project (HAP-MAP) (24, 39). For measured HAPs with documented cancer toxicity metrics, we translate ambient concentrations into cancer risk estimates, the sum of which is the total (or cumulative) cancer risk estimate. We first present an analysis of 2020 AirToxScreen data to contextualize our study: we illustrate the magnitude of current USEPA cancer risk estimates (from all 72 HAPs with cancer risk estimates modeled by AirToxScreen), the spatial variability of those estimates, and which chemicals drive total cancer risk estimates in the corridor. Next, using mobile lab concentration data, we present cancer risk estimates from the 17 HAPs we measured for 15 census tracts and compare our measured estimates against those modeled in AirToxScreen.

Results

Cancer Risk Estimates from AirToxScreen Data. Air pollution cancer risk for a given carcinogen is estimated by multiplying the lifetime exposure concentration by the IUR value. AirToxScreen cancer risk estimates are based on modeled exposure concentrations and IUR values listed in USEPA Integrated Risk Information System (IRIS) database (40). We use these same IUR values for estimating cancer risk from our measured concentrations (presented in the following section). AirToxScreen provides cancer risk estimates for 72 individual HAPs, including primary and secondary VOCs and particulate metals.

To contextualize our measurements, we first present an analysis of AirToxScreen risk estimates for the BR-NO corridor (outlined in green on map in Fig. 1A), which consists of 530 total census tracts. Fig. 1A shows a map of total estimated cancer risk from AirToxScreen for the BR-NO corridor at the census tract level. Nearly all (97%) of the 530 census tracts in the BR-NO corridor are above the 50th percentile nationwide for total cancer risk. Within the corridor, there are many areas of very-high risk relative to the rest of the country: 32% of corridor tracts are above the 95th percentile nationwide, and 7% of corridor tracts are above the 99th percentile. Two census tracts (0.4% of total

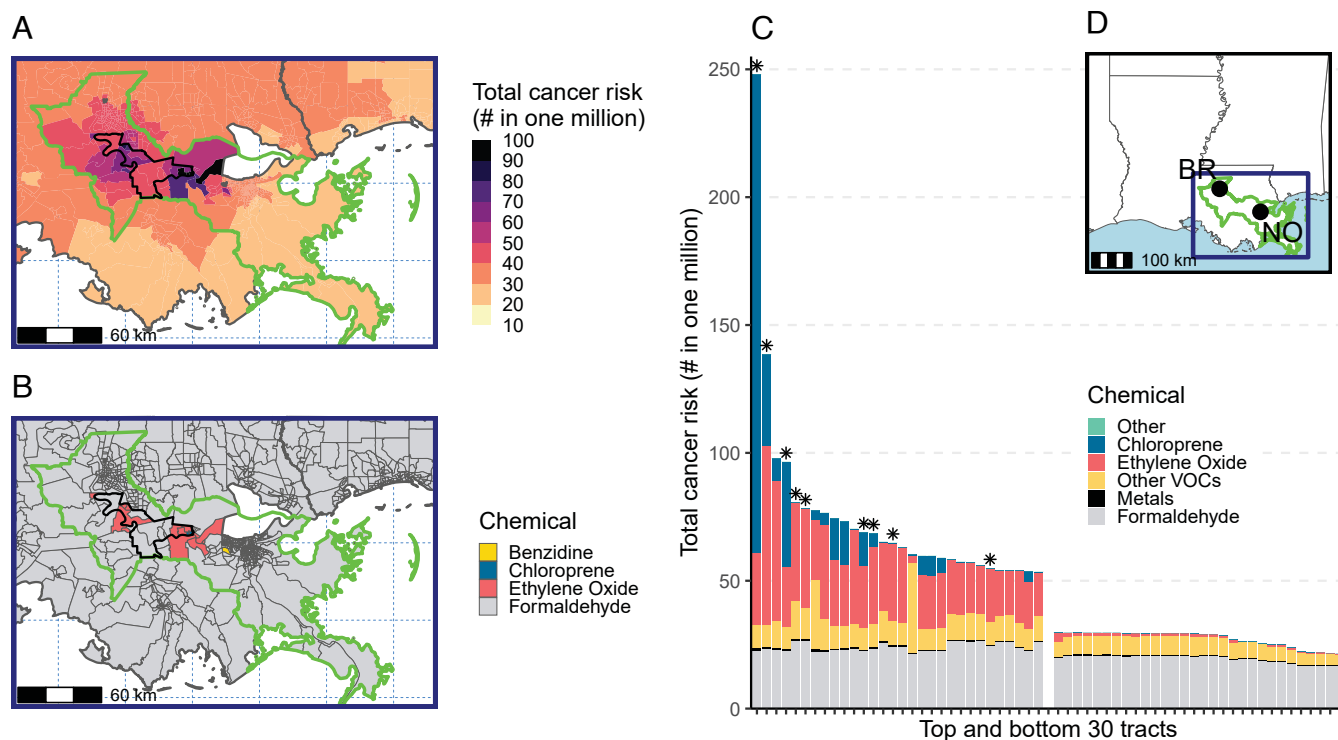


Fig. 1. Using AirToxScreen to understand potential cancer risk in southeastern Louisiana. (A) Map of total estimated cancer risk from AirToxScreen by census tract. The entire industrial corridor is outlined in green, and the 15 census tracts where we made measurements are outlined in black. (B) Map showing which HAP has the single highest individual cancer risk, as estimated in AirToxScreen. (C) Bar chart showing total risk (height of bar) and relative contributions by chemical category for the census tracts within the industrial corridor with the 30 highest and lowest total risk estimates. The subset of bars with star symbols (“*”) above are those where we made ambient measurements. Nine of the 15 tracts in which we made measurements are in the top 30 highest risk tracts in the corridor, per AirToxScreen. (D) Inset map of state of Louisiana showing the outline of the industrial corridor (green) and the spatial extent of the two maps on the left (navy blue box). Baton Rouge (“BR”) and New Orleans (“NO”) are indicated on the map.

in corridor) have estimated tract-level cancer risk above the maximum “acceptable” level of cancer risk advised in USEPA Superfund Site remediation of 100-in-one million (41). Many tracts have levels of cancer risk just below this “acceptable” threshold as well: For example, 40 tracts (7.5% of total in corridor) have risk levels higher than 50-in-one million.

Despite AirToxScreen identifying the area as a clear hot spot for cancer risk, there is still a large degree of spatial variability in total cancer risk estimates at the census tract level. This variability spans an order of magnitude across the corridor, which is shown in Fig. 1A. The tract with the highest cancer risk estimate was 248-in-one million, and the lowest was 21-in-one million. This variability is the result of substantial spatial variation in individual HAPs concentrations and associated risk. Fig. 1B shows a map of census tracts colored according to which HAP has the single largest individual risk estimate for that tract. Four different HAPs are shown as having the largest individual contribution to total cancer risk for these tracts: formaldehyde, ethylene oxide, chloroprene, and benzidine.

For a large majority (95%) of tracts in the BR-NO corridor, formaldehyde has the highest individual contribution to total risk of all HAPs. Formaldehyde is linked to nasal cancers and myeloid leukemia (31). Statewide, an even higher percentage (97%) of all tracts have formaldehyde as the largest contributor to risk (SI Appendix, Fig. S2A). However, the magnitude of formaldehyde-attributed cancer risk is relatively uniform across the corridor; the full range spans only a factor of 1.59 (17- to 26-in-one million risk). Formaldehyde’s uniformity is explained by its formation largely from secondary photochemical and biogenic sources, not specifically industrial primary emissions

(42). Despite the homogeneity within the corridor, AirToxScreen estimates of formaldehyde cancer risk are more variable statewide (SI Appendix, Fig. S2D), and the highest-estimated formaldehyde risk is outside of the industrial corridor entirely; indeed the maximum formaldehyde risk in the corridor only corresponds to the 37th percentile statewide.

Ethylene oxide is the largest individual contributor to total cancer risk for 14 total tracts in the corridor (3% of tracts). Ethylene oxide is thought to be a primary-only pollutant largely from industrial point sources and is linked to lymphoid and breast cancers (29). The tracts with ethylene oxide as the largest contributor include parts of four different parishes (Ascension, Iberville, St. Charles, St. John the Baptist), with a maximum individual tract contribution of 70-in-one million, corresponding to an exposure concentration of roughly 8 ppt. The high-ethylene oxide tracts cover a large fraction of the area (~1,000 km²) of the BR-NO corridor. There are additionally five tracts outside of the BR-NO corridor where ethylene oxide is the highest single contributor to total cancer risk, each of which are in the Lake Charles area where there are multiple known industrial emissions sources (SI Appendix, Fig. S2A).

Chloroprene is the largest contributor to cancer risk for two tracts, both of which are in St. John the Baptist Parish, home to the only major production facility of chloroprene in the United States, which accounts for 96% of nationwide emissions according to TRI (year 2022). Chloroprene is a monomer used for the production of polychloroprene rubber (trade name e.g., “Neoprene”), a synthetic rubber material used in a variety of applications (e.g., protective and orthopedic garments, gaskets, and seals, etc.) due to its with high physical flexibility and

resistance to water and heat (30, 43). These tracts and the area around this facility are essentially the only place where cancer risk is attributed to chloroprene in the state, though the magnitude of risk in these tracts is very high. The maximum tract-level risk value for chloroprene is 187-in-one million, which is the highest tract-level value for any chemical in the BR-NO corridor in AirToxScreen estimates. Chloroprene is linked to a wide variety of cancers, including leukemia and those affecting the liver and lungs (30).

Benzidine [IUR = $6.7 \times 10^{-2} \mu\text{g m}^{-3}$ (44)] is the largest contributor to risk for one tract (tract ID: 22051027501), which is in Jefferson Parish. The benzidine-attributed risk in this tract is only slightly higher than that of formaldehyde (25- vs. 21-in-one million, respectively). This level of risk corresponds to very low concentration (<1 ppt), due to the very high IUR value for benzidine.

Fig. 1C shows that the spatial variation of chloroprene- and ethylene oxide-attributable cancer risk are high relative to formaldehyde, which is comparatively invariable across the corridor. We group these chemicals into categories in Fig. 1C, where formaldehyde, chloroprene, and ethylene oxide each comprise their own category, while all particulate metals are listed in the “Metals” category and all other VOCs are in the “Other VOCs” category. We see that tracts with the highest estimated total cancer risk have varying, but substantial, contributions from both chloroprene and ethylene oxide, or from ethylene oxide alone.

Based on AirToxScreen estimates, formaldehyde, ethylene oxide, and chloroprene together account for the large majority of total cancer risk in the BR-NO corridor, especially for those tracts with the highest levels of total risk. For the 30 tracts with the highest risk estimates (Fig. 1C), the relative contribution of the sum of formaldehyde, chloroprene, and ethylene oxide to the total ranged from 41 to 96%, with a median value of 84%. The tract with only 41% of the risk being attributed to these three chemicals is an outlier, as it has a much-larger risk attributed to Other VOCs compared to the other tracts. This is the tract discussed above (tract ID: 22051027501), where benzidine has the single highest risk estimate and also makes up the large majority of risk from the Other VOCs category.

Conversely, those tracts in the corridor with the lowest cancer risk estimates (e.g., the lowest 30 tracts, Fig. 1C) have very little risk attributed to ethylene oxide relative to formaldehyde and essentially none attributed to chloroprene. Formaldehyde dominates the total risk estimate, contributing on average 71% to the total risk. Formaldehyde-attributed cancer risk across these low-risk tracts, however, is only 19% lower on average than it is for the high-risk tract. Again, this owes to relatively uniform regional background concentrations from photochemical production.

The median relative contribution to total cancer risk for all other VOCs across the corridor was 15% and for metals was 0.6%. All individual risk estimates for Other VOCs in AirToxScreen were below 5-in-one million level of risk, and all individual risk estimates for metals were below 1-in-one million level of risk. The relative contribution for these two categories is roughly similar between the high- and low-risk tracts, with the exception of a few tracts with high relative contributions from Other VOCs, as discussed above. While this paper does not contain any metals measurements, nor the comprehensive set of VOC HAPS measurements treated by AirToxScreen, we will show in the next section that AirToxScreen modeled concentrations can dramatically underestimate actual measured concentrations, which is an argument for targeted sampling even for species and/or areas not highlighted as high-risk in AirToxScreen.

Cancer Risk Estimates from Measurements and Comparison with AirToxScreen. Using advanced instrumentation aboard a mobile laboratory during February 2023, we measured a large suite of HAPs in the heart of the BR-NO industrial corridor. Seventeen of these VOC HAPs are known carcinogens, and we use their measured concentrations to present the associated cancer risks here. In a previously published mobile monitoring study, we aggregated ethylene oxide measurements into representative concentrations for 500 m \times 500 m grid cells and at the census tract level (39). We apply similar spatiotemporal aggregation methods here to the rest of the carcinogenic air pollutants that we measured, and use these representative concentrations as the basis for our cancer risk estimates, assuming that they represent lifetime exposure concentrations. Table 1 contains the full list of measured compounds and their IUR values used for risk calculations. Details of our spatiotemporal aggregation methods are provided in *Materials and Methods*.

Fig. 2 illustrates the magnitude of total and individual estimated cancer risk for the 15 census tracts where we made measurements. Fig. 2A illustrates how each measured HAP category contributes to the cumulative risk of each tract, with the corresponding estimate from AirToxScreen for comparison. Note that our cancer risk estimates are derived from the 17 HAPs we measured, but we compare to all 72 HAPs with modeled cancer risk in AirToxScreen. We also show the average across all 15 tracts for both measured risk and AirToxScreen. These tracts span parts of four parishes (see *Inset* map in Fig. 2B). Fig. 2C presents similar information but shows the number of census tracts with measured estimates of risk that are above different thresholds, both for risk from individual HAPs and total.

Like AirToxScreen, we find that formaldehyde, chloroprene, and ethylene oxide drive the large majority of the total cancer risk (range: 62.6 to 96.2%). However, for all tracts but one, our estimates were larger than AirToxScreen (range: 1 to 11.7 \times ; median: 5.1 \times). The median tract-level cancer risk from our measurements was 310-in-one million, compared to 60-in-one million for AirToxScreen, and the maximum tract-level risk estimates were 560-in-one million and 250-in-one million, respectively.

The total cancer risk estimates shown in Fig. 2A are mapped in Fig. 3. We see that the tracts in the northwest corner of our sampling domain (parts of Iberville and Ascension parishes) had the highest total cancer risk. The middle of our sampling domain had total cancer risk values on the lower side of this distribution (parts of St. James Parish), and then the southeastern part of the domain had higher values as well (parts of St. James and St. John the Baptist parishes) though not as high as the northwestern-most tracts. *SI Appendix, Fig. S5* contains a map with both our tract-level total risk estimates and those for 500 m \times 500 m grid cells, which illustrates that there can be substantial within-tract variability of total risk as well, with some locations having substantially higher risk levels than the tract average. AirToxScreen estimates had a different spatial pattern compared to our tract-level estimates. For AirToxScreen, the highest-risk tracts were in the southeastern part of the domain (St. John the Baptist parish) and have elevated chloroprene and/or ethylene oxide concentrations relative to the other tracts, as discussed above.

Formaldehyde and Other VOCs contribute roughly equally to total cancer risk, with mean values of 23.9- and 39.4-in-one million, respectively. These estimates represent an average of 8.4% (range: 4.1 to 14.3%) and 10.5% (range: 3.8 to 37.4%) of the total cancer risk we estimate across all tracts.

Table 1. HAPs measured in this study and related info, including the IUR values used and whether we applied age-dependent adjustment factors (ADAFs) to IUR values

HAP	Category	Instrument	IUR (per $\mu\text{g m}^{-3}$)	ADAF
Ethylene Oxide	Ethylene Oxide	TILDAS	5.0e-03	Y
1,2-dibromoethane	Other VOCs	GC-EI-ToF	6.0e-04	—
Chloroprene	Chloroprene	GC-EI-ToF	5.0e-04	Y
Butadiene	Other VOCs	GC-EI-ToF	3.0e-05	—
1,2-dichloroethane	Other VOCs	GC-EI-ToF	2.6e-05	—
Chloroform	Other VOCs	GC-EI-ToF	2.3e-05	—
1,1,2-trichloroethane	Other VOCs	GC-EI-ToF	1.6e-05	—
Formaldehyde	Formaldehyde	TILDAS	1.3e-05	—
Vinyl chloride	Other VOCs	GC-EI-ToF	8.8e-06*	Y
Benzene	Other VOCs	GC-EI-ToF	7.8e-06†	—
1,4-dioxane	Other VOCs	GC-EI-ToF	5.0e-06	—
Trichloroethylene	Other VOCs	GC-EI-ToF	4.8e-06	Y
1,3-dichloropropene	Other VOCs	GC-EI-ToF	4.0e-06	—
Acetaldehyde	Other VOCs	GC-EI-ToF	2.2e-06	—
Bromoform	Other VOCs	GC-EI-ToF	1.1e-06	—
Tetrachloroethylene	Other VOCs	GC-EI-ToF	2.6e-07	—
Dichloromethane	Other VOCs	GC-EI-ToF	1.7e-08	Y

*We use the “Continuous lifetime exposure from birth” IUR for vinyl chloride instead of applying an ADAF to an adult-based lifetime exposure.

†We use the upper value of the range of EPA IRIS IUR values for benzene, similar to AirToxScreen.

For all tracts, Other VOCs had larger measured risk estimates compared to AirToxScreen, and formaldehyde-associated risk between measurements and AirToxScreen was very similar.

There was little spatial variability in the risk attributed to formaldehyde from our measurements, which is similar to AirToxScreen. The relative SD (RSD), which is the SD divided by mean, in estimated cancer risk from measurements and AirToxScreen were 0.074 and 0.058, respectively. As discussed more fully in *Materials and Methods*, we applied a “seasonal correction factor” to our formaldehyde measurements in an

effort to better represent an annual average, as formaldehyde concentrations exhibit strong seasonality (due to photochemical production) and our measurements were taken during winter. All AirToxScreen concentration estimates are annual averages.

Spatial variability was higher for Other VOCs compared to formaldehyde. The RSD in Other VOCs in AirToxScreen risk estimates was 0.2, while the RSD from measurements was considerably higher (1.273). We measured a few outlier tracts (e.g., “B,” “C,” and “D” in Fig. 2B) that had high risk; RSD was 0.361 with these tracts removed from the calculation. There is a

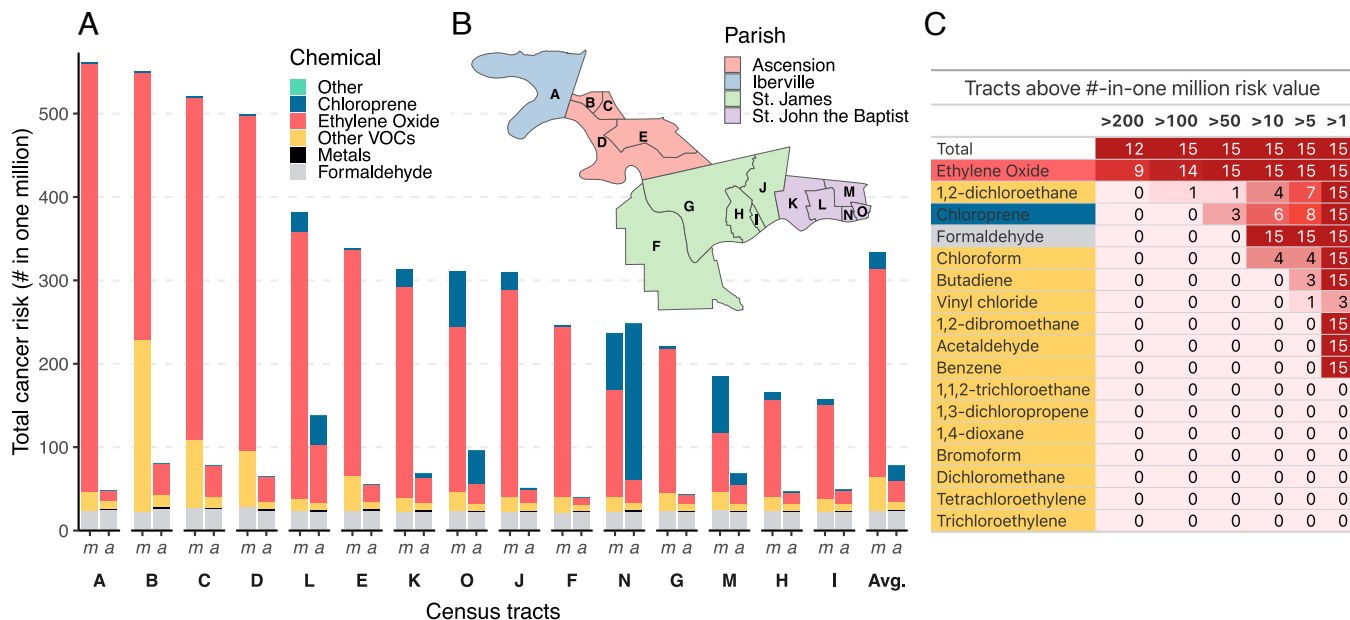


Fig. 2. Measured estimates of cancer risk. (A) Total cancer risk estimates from measurements and total cancer risk estimates from AirToxScreen. Each pair of bars refers to one of 15 census tracts, with the letter below corresponding to the labeled *Inset* map in panel (B) as well as the average across all tracts. Each bar is sub-labeled with *m* or *a* to indicate whether the risk estimate is from measurements or AirToxScreen, respectively. Bars are ordered by descending estimates of total cancer risk from measurements. (C) Table showing the cancer risk estimate from measurements associated with each HAP. Numbers in the table indicate how many of the 15 census tracts correspond to different levels of cancer risk, per HAP. Colors in the left-most index row correspond to the same category coloring scheme in panel (A).

Downloaded from https://www.pnas.org by 70.174.248.45 on October 7, 2025 from IP address 70.174.248.45.

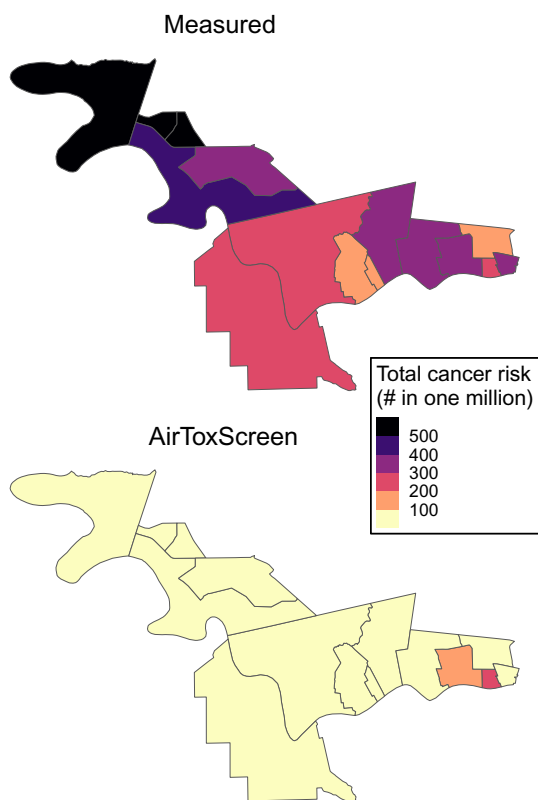


Fig. 3. Map of total cancer risk estimates from measurements (*Top*) and AirToxScreen (*Bottom*).

very high degree of variability within the Other VOCs category as to which specific chemicals drive risk across these tracts, reflecting the large number of different industrial emissions sources in the area. Risk in the Other VOCs category for these outlier tracts, for example, is driven by high levels of 1,2-dichloroethane and, to a lesser extent, chloroform. For example, the risk attributed to 1,2-dichloroethane in tract “B” corresponds to 174-in-one million. This example is important to highlight because the risk is well above the unacceptable threshold but is not highlighted in AirToxScreen at all as a HAP of concern in the area.

Chloroprene and ethylene oxide cancer risk estimates from our measurements are more spatially heterogeneous than the Other VOCs category. The observed spatial variation for chloroprene and ethylene oxide is expected of primary pollutants with major industrial sources in the area, in contrast with VOCs dominated by secondary production (e.g., formaldehyde). The RSD in measured risk estimates for chloroprene and ethylene oxide are 1.317 and 0.505, respectively.

For chloroprene, measured concentrations were high in the vicinity of the major emissions source, and below the instrumental limit of detection elsewhere (*SI Appendix, Fig. S6A*). The maximum tract-level cancer risk for chloroprene from our measurements was 68-in-one million, while for AirToxScreen it was 187-in-one million. We estimate that chloroprene contributes 7.9% on average to total cancer risk for those tracts in our sampling domain, but the relative contribution varied widely (range: 0.2 to 36.3%)

There are a mix of tracts where AirToxScreen cancer risk estimates for chloroprene are larger than our estimates (e.g., “L”, “N” from Fig. 2*A*) and vice versa (e.g., “M”, “O”). However, the broad spatial pattern of chloroprene risk across the domain for the two estimates is similar, with a high-to-low gradient of values

moving west away from the single major point source located in the easternmost part of the domain (see *SI Appendix, Fig. S6* for grid cell and tract-level maps of chloroprene concentration and risk). The magnitudes of the two risk estimates were relatively similar for each tract (*SI Appendix, Fig. S4*), and the discrepancies can be explained by inaccuracy in underlying emissions estimates and/or potential spatiotemporal sampling bias.

Ethylene oxide, while spatially heterogeneous like chloroprene and unlike formaldehyde, represents a much larger fraction of the total cancer risk we estimated compared to AirToxScreen. The maximum tract-level cancer risk for ethylene oxide from our measurements was 515-in-one million compared to 70-in-one million from AirToxScreen. There are multiple ethylene oxide hot spots that we identified with our mobile lab (e.g., in both the northwest and southeast portions of the domain), owing to the much-larger (compared to chloroprene) number of emissions sources in the vicinity. 12 of 14 TRI-listed ethylene oxide emitters in the state are in the BR-NO industrial corridor, and 10 of those are within 11 km of our sampling route.

AirToxScreen identifies ethylene oxide as an important, but not dominant, chemical driving cancer risk in the region. Our measurements, on the other hand, identify ethylene oxide as contributing a large majority (average: 73.2%, range: 39 to 91.7%) of the total risk in the area. Some of this discrepancy is due to an ethylene oxide background concentration of zero in AirToxScreen, while our measurements suggest an area background concentration that corresponds to roughly 200-in-one million cancer risk, which we discuss further in the next section. With the exception of one tract (“N,” which has a high contribution from chloroprene), the risk we estimate from ethylene oxide alone is larger than the total risk estimate from AirToxScreen for all other tracts.

The table in Fig. 2*C* facilitates comparison of the spatial extent of impacts between different HAPs. Ethylene oxide is almost uniformly above 100-in-one million levels of risk, while formaldehyde is uniformly between 10- and 50-in-one million levels of risk. 1,2-dichloroethane is the only other VOC we measured which had risk above 100-in-one million anywhere, which it did for one tract. Additionally, three and four tracts for 1,2-dichloroethane and chloroform, respectively, were between 10- and 50-in-one million levels of risk, highlighting that other VOCs do contribute meaningfully to cumulative risk. A number of the chemicals we measured (the bottom seven entries in this table), had risk levels less than 1-in-one million across all tracts in the domain.

Discussion

We find that the cumulative cancer risks determined from ambient concentration measurements of 17 HAPs across 15 census tracts in the BR-NO corridor exceed USEPA’s suggested risk threshold of 100-in-one million. This cancer risk is unacceptably high, especially for an area with high social and economic vulnerabilities. Additionally, we show that ethylene oxide, chloroprene, and formaldehyde contribute the large majority of the cumulative cancer risk across the tracts in which we performed mobile measurements. Of these HAPs, ethylene oxide is the single most important driver of risk.

Our analysis of AirToxScreen risk estimates also identified these three chemicals as the main drivers of risk for this area; however, the total cancer risk estimates in AirToxScreen are much lower than what estimates from measured concentrations indicate. Within the BR-NO corridor, none of the LDEQ

monitoring stations report measurements of ethylene oxide, chloroprene, or formaldehyde. Thus, the cancer risk estimates we provide using our mobile measurements are the most spatiotemporally comprehensive risk estimates for this region to date.

Chloroprene, notably, is measured routinely by the company that owns and operates the chloroprene production facility near LaPlace, Louisiana. The genesis of this monitoring was undertaken in large part because the modeled concentrations and risk levels in 2011 National Air Toxics Assessment (NATA, now named AirToxScreen) were extremely high (45). Indeed, these monitoring efforts, which began in 2016, have shown that chloroprene concentrations in LaPlace correspond to excessive cancer risk, even higher than the high modeled AirToxScreen concentrations that triggered the monitoring efforts to begin with. Over time, they have also reflected the implementation of emissions controls, as measured chloroprene concentrations have been in decline in recent years since this monitoring began (*SI Appendix, Fig. S8*). Similarly, the 2020 AirToxScreen identifies ethylene oxide as a key HAP that is responsible for high cancer risk, as the 2011 NATA did for chloroprene. And like for chloroprene, our measurements show that actual ethylene oxide concentrations correspond to unacceptable risk levels, which are significantly higher than AirToxScreen estimates.

Indeed, the main discrepancy between our total cancer risk estimates and those in AirToxScreen is from underestimated ethylene oxide concentrations in AirToxScreen. The median tract-level ethylene oxide concentration we measured is 27.7 ppt, with a maximum of 57.2 ppt, while the median and maximum from AirToxScreen are 2.6 ppt and 7.8 ppt, respectively (39). Under the assumption that tract-level concentration estimates represent lifetime exposures, these concentration differences represent large differences in estimated cancer risk. Even the lowest tract-level ethylene oxide cancer risk estimate is larger than the total risk estimate from AirToxScreen for 10 of 15 tracts. The cancer risk attributable to ethylene oxide alone is larger than 100-in-one million risk for 14 of 15 tracts.

The measurement of ethylene oxide in ambient air, particularly in areas not directly associated with point sources, is an active area of research (46). There are considerable unknowns regarding both sources and potential atmospheric transformations of ethylene oxide. While the USEPA has undertaken nationwide ethylene oxide monitoring, interpretation of that dataset is complicated by multiple potential measurement artifacts, such as coelution and mass spectral overlap (47), as well as in-canister formation of ethylene oxide under certain circumstances (48). Perhaps reflecting this lack of information, an ambient background concentration of ethylene oxide of zero is asserted in AirToxScreen. As detailed by Robinson et al. (39), we measured 22 ppt at the stationary measurement site near Donaldsonville, LA, which corresponds to a cancer risk value of 200-in-one million, and showed that this area was relatively unimpacted by detectable plumes, unlike many near-source locations on our mobile sampling route where we saw intermittent high-concentration plumes. This was roughly the same as the median grid cell concentration from mobile monitoring, for cells that were not within 1 km of any industrial facility. These data indicate that a background greater than 0 is present, and contributes substantially to the overall cancer risk shown in Figs. 2 and 3.

We found the potential spatial sampling bias in our tract-level ethylene oxide concentration estimates to be negligible (see ref. 39), and, if anything, hypothesize that temporal sampling bias likely minimizes the true discrepancy with the AirToxScreen

comparison in the following ways: first, in comparing our measured risk estimates to AirToxScreen, we are comparing to a representation of the year 2020, which uses emissions estimates from that year. Estimated ethylene oxide concentrations and associated risk, however, have been steeply declining in recent AirToxScreen assessments (*SI Appendix, Fig. S7*). It stands to reason that an AirToxScreen assessment for year 2023 likely would contain lower estimates of risk attributable to ethylene oxide. Second, there is a small, but suggestive amount of emerging evidence that ethylene oxide ambient concentrations exhibit a seasonality with higher concentrations in summer compared to winter (46, 49–51). This potential trend and currently unknown underlying mechanism are uncertain enough that we did not perform a seasonal correction for ethylene oxide as we did for formaldehyde; however, such seasonality would suggest that our February concentration measurements may be lower than an annual average.

Similarly, the decline in ambient chloroprene concentrations in recent years (discussed above) very likely means that 2020 AirToxScreen estimates are higher than they would be for AirToxScreen for year 2023, which would be more directly comparable to our measurements. In the cases of both chloroprene and ethylene oxide, the declining trend in measured and/or estimated concentrations is important context for considering what the actual lifetime exposures to these chemicals may be for residents in the area, as the true risk from exposures over a longer timeframe may be higher than what we assume here.

The lone tract in Fig. 1*B* where benzidine was identified as the single highest contributor to risk from AirToxScreen estimates is an interesting case, though we did not measure benzidine in this project nor make any measurements within that particular tract. Reported benzidine emissions from a landfill (17) in Jefferson Parish explain the high risk estimates attributed to it in this and neighboring tracts; benzidine emissions at this site increased 11× from 2019 to 2020 AirToxScreen (15, 52). Concentrations (and associated risk) were near zero in 2019 AirToxScreen. Benzidine is not found in nature but was used widely in the past as a dye, though has not been manufactured or actively used in the United States for decades (53). It is linked to bladder cancer (44). Thus, these benzidine emissions may represent something of a “one-off” disposal event, but also emphasize potentially large number of HAPs that people living near landfills may be exposed to.

As mentioned in the introduction, LDEQ operates VOC HAPs monitoring sites ($n = 10$) in the wider industrial corridor, two of which are within 5 km of our sampling route. Neither of the two sites closest to our sampling route had total cancer risk estimates above 40-in-one million; we used February 2023 average concentrations for all compounds measured at each site to calculate risk (*SI Appendix, Fig. S10*). LDEQ measures 16 carcinogenic HAPs, six of which are common to the list of HAPs that we present risk estimates for (1-1-2-Trichloroethane, 1-2-Dichloroethane, Benzene, Butadiene, Chloroform, and Vinyl Chloride). The chemical with the single largest contribution to risk at either of these two LDEQ measurement sites was acrylonitrile (10-in-one million), an important commodity chemical used in the production of nylons, acrylamide, and acrylic acid. We should note that acrylonitrile is categorized in IRIS as a “probable human carcinogen” based on limited evidence of carcinogenicity in humans, but because it is included in AirToxScreen, we include it here as well (54). We did not consider acrylonitrile in our own measurement-based analysis, though the maximum tract-

level risk attributed to acrylonitrile in AirToxScreen within our sampling domain is less than 2-in-one million.

We also calculated cancer risk using 2023 annual average VOC concentrations for all of the 10 LDEQ sites corridor-wide. Here, we see that two sites (not those closest to our sampling route) exceed 100-in-one million risk, with acrylonitrile dominating the risk estimate at each site, accounting for >87% of the total (*SI Appendix, Fig. S11*). While the LDEQ monitoring sites do not provide a point of comparison for ethylene oxide, chloroprene, or formaldehyde-related risk, they do highlight that acrylonitrile is a potentially important HAP shaping risk in the region. Looking at the LDEQ monitoring data in concert with our own mobile measurements only reinforces the idea that risk estimates can be highly spatially variable in a densely industrialized region like this one and that total risk estimates are strengthened by measuring a comprehensive list of HAPs. It also provides another instance where measured risk estimates far exceed those from AirToxScreen. These discrepancies make clear the need for comprehensive, accurate ambient measurements of HAPs to serve as ground-truthing indicators of risk and for improved model estimates that explore different emissions scenarios and compare to ambient measurement data sources.

We show clearly that a cumulative risk framework is important and necessary for an area like the BR-NO corridor that has many different primary HAPs emissions sources. Even when individual HAPs have ambient concentrations corresponding to “acceptable” levels of risk (e.g., formaldehyde) there are likely to be other HAPs present that, cumulatively, may present higher-than-acceptable levels of total risk. Any evaluation of emissions sources that only considers the individual risk from a HAP in the context of acceptability thresholds will underestimate the actual burden of cancer risk to nearby communities. Our measurements show that these communities are facing higher-than-acceptable total levels of cancer risk.

Materials and Methods

Mobile Monitoring. We measured concentrations of a suite of 17 VOCs used in this risk analysis. These measurements were made aboard the Aerodyne Mobile Laboratory (AML), which has been described in detail elsewhere (37, 55). In brief, the AML consists of a large step-utility van that hosts real-time gas- and particle-phase pollutant instruments. Further details about the AML inlet, inlet lag correction, and instrument flow rates used in this campaign are provided in *SI Appendix* of Robinson et al. (39). The ethylene oxide measurements used for this risk analysis are previously published by Robinson et al. (39), while the rest of these measured concentrations are presented here for the first time. Many of the chemicals we measured are almost exclusively measured using off-line, integrated sampling. Real-time, in situ chemical detection allows for resolving pollutant concentrations across space using a mobile platform. However, there are likely additional health relevant chemical species that are not easily measured by existing instrumentation and require continued development of advanced measurement technologies.

Our experimental design aimed to provide spatially resolved representative concentrations of air pollutants across the region to be used as the basis for risk assessment. We designed a driving route that passed by as many industrial facilities as possible, while still being manageable to complete at least once per day. We used facility locations from the TRI and assumed a typical AML speed of 40 km per hour to create four driving “loops,” or sections, which we drove at least once per driving “shift” over the course of the month-long campaign. Previous mobile monitoring studies (34, 56–58) have shown that repeatedly capturing measurements of an air pollutant at a location can provide long-term representative concentrations for that location given a sufficient number of visits. We parked the AML during down-time from mobile sampling at an RV parking

lot (coordinates: 30.0890, –90.9344) near Donaldsonville, LA (referred to as the “stationary site”). We staggered our departure time from the stationary site each day, as well our driving direction, in an effort to minimize bias related to diurnal patterns. The driving route passed through 15 census tracts in parts of four parishes. Full details about the driving route, the sampling schedule, a typical driving shift, and spatial and temporal data coverage are provided in *SI Appendix* of Robinson et al. (39).

Chemical Measurements.

TILDAS (ethylene oxide and formaldehyde). Two dedicated tunable infrared laser direct absorption spectrometers (TILDAS; Aerodyne Research, Inc.) were used for measuring ethylene oxide (50) and formaldehyde (59, 60). Each instrument has a sub-1 Hz native response time and collected data at 1 Hz time resolution. Both instruments were spectrally backgrounded using either ultrazero air (for formaldehyde) or humidity-matched scrubbed air (for ethylene oxide).

The version of the ethylene oxide TILDAS used here (TILDAS-FD-ETO) employs a 413 m path length cell, and measures in the 3065.55 to 3066.10 cm^{-1} region. This region also includes absorption of other key species like H_2O , C_2H_6 , HCHO , C_2H_4 , CH_4 , and CH_3OH , all of which are accounted for with custom spectral fitting software (“TDLWintel;” Aerodyne Research, Inc.). Instrument detection limits (estimated as $3 \times \text{SD}$) are 186 ppt for 1-s mobile data, and 45 ppt for 100-s stationary data. We estimate a 25% overall uncertainty for all measured ethylene oxide mixing ratios, due to uncertainties in gas standards and calibration error. Additional details on operation, calibration, and inlets for the ethylene oxide TILDAS are provided in *SI Appendix* of Robinson et al. (39).

The formaldehyde TILDAS has a 76 m path length cell, and measures in the 1764.1 to 1765.5 cm^{-1} region. It has 2-s mobile and 100-s stationary detection limits of 130 and 690 ppt, respectively. We estimate 5 to 10% overall uncertainty for the formaldehyde TILDAS, based on the uncertainty in the spectral line in the HITRAN (high-resolution transmission molecular absorption) database (61). As described in a following section, we use a seasonal correction factor to adjust the aggregated formaldehyde mixing ratios to represent annual averages. Additional details on operation, calibration, and inlets for the formaldehyde TILDAS can be found in *SI Appendix*.

GC-MS (chloroprene and other VOCs). All VOC species other than formaldehyde and ethylene oxide, including chloroprene, were measured by an in situ coupled gas-chromatograph-mass spectrometer (GC-MS) that uses electron ionization and is equipped with a high-resolution time-of-flight MS. The full list of measured species used in this risk analysis is shown in Table 1. This GC-MS system has been described fully by Claffin et al. (62). Briefly, the system uses thermal desorption preconcentration (TDPC) followed by injection into a two-channel GC column for separation. Channel 1 was equipped with a porous layer open tubular (PLOT) column (Restek 15 m PLOT MXT-Q-Bond) for separating high-volatility species (e.g., C_2 – C_5 hydrocarbon, C_1 – C_3 oxygenated VOCs), while Channel 2 utilized a nonpolar column (Restek 30 m Rxi-624MS) for separating mid-volatility VOCs (C_5 – C_{12} hydrocarbon, C_2 – C_{10} oxygenated VOCs).

We operated the GC-MS on a 30-min duty cycle with 10-min sample collection per half-hour and a 20-min sample prep, separation, and detection. GPS data were matched to the 10-min sample collection portion of each cycle for subsequent spatial analysis. The instrument demonstrates typical LODs of 1 ppt, and reports speciated VOCs with an estimated 30% uncertainty.

For some samples, the GC-MS software did not report values, and in these cases, we have imputed data with the value of $\text{LOD}/\sqrt{2}$ (63). Nonreported values correspond to one of two conditions: either no chromatographic peak was present, and so no peak could be fit, or a peak was able to be fit due to a peak being above the noise of the instrument baseline, but the calculated concentration was below the typical LOD, and so no value was reported. Imputing the data with $\text{LOD}/\sqrt{2}$ assumes that these periods correspond to sub-LOD concentrations.

Spatial Data Analysis. We performed a data reduction on the time-series for each pollutant that is conceptually similar to that described by Apte et al. (34), aiming to produce mixing ratios resolved across space. This procedure is detailed fully in ref. 39 for the already-published ethylene oxide data. In brief, all raw measurements are aggregated into grid cells (500 m \times 500 m). Data in a given

grid cell collected within a unique hour are grouped together as a "visit," and the mean of those data give a "visit mean." The overall grid cell value is the mean of all visit means.

We estimate census tract-level mixing ratios as the areal average of all within-tract grid cell values. Grid cells whose centroids are within a given census tract are matched to that tract. Tract "F" shown in Fig. 2 (Tract ID: 22093040500) contained our stationary site, and we base our estimates for this tract solely on the measurements collected while the AML was stationary. This tract only contained a small number of grid cells in which we made measurements, much of which were on the Sunshine Bridge, and so using the long-term average from the stationary site is most appropriate for this tract.

Our tract-level concentration (and accompanying risk) estimates are based on our grid cell concentration estimates, which necessarily cover only a subset of each census tract due to the sparse road network and private property. AirToxScreen tract-level estimates, on the other hand, are true areal averages across the entire census tract derived from gridded (subtract) modeling estimates. We assessed the potential spatial sampling bias in our tract estimates relative to those in AirToxScreen for the case of ethylene oxide in ref. 39 and concluded that bias appears minimal. This same pattern is likely true for chloroprene as well and is likely unimportant for the case of formaldehyde. Thus, we expect our sampling to be relatively free of spatial bias, at least for these pollutants with the largest contributions to total risk.

Last, we define the BR-NO industrial corridor using parish boundaries for those parishes along the Mississippi River in which industrial facilities are clustered. The full list includes Ascension, Assumption, St. Bernard, East Baton Rouge, West Baton Rouge, St. Charles, St. John the Baptist, St. James, Iberville, Jefferson, Orleans, and Plaquemines. All spatial analysis was performed using the sf: Simple Features for R GIS library (64), and all maps were made using the ggmap R library (65).

Cancer Risk Assessment. Cancer risks associated with exposure to a chemical in air are assessed using an IUR, which provides an upper-bound estimate of the increased cancer risk from continuous exposure to a chemical in air at a concentration of $1 \mu\text{g m}^{-3}$. To calculate cancer risk estimates based on measured ambient concentrations, we searched the IRIS database (40) for IURs and mode of action information for the 17 measured chemicals (Table 1). For chemicals with a mutagenic mode of action (e.g., ethylene oxide, chloroprene), we used ADAFs to adjust the IUR to account for the higher expected carcinogenic risks incurred with early-life exposures (66). As detailed in a previous section, for each chemical we multiplied the measured census tract-level concentration by its IUR value to calculate excess lifetime cancer risks (i.e., the incremental probabilities of developing cancer over a lifetime as result of exposure). To estimate total excess cancer risks associated with exposures to the mixture of chemicals found in each census tract we added together all calculated excess lifetime cancer risks in accordance with USEPA methodology. A key assumption of this analysis is that the ambient concentrations we report for census tracts represent exposure concentrations that are consistent over a lifetime.

AirToxScreen calculates cancer risk in the same way, though uses modeled exposure concentrations that are distinct from modeled ambient concentrations. Exposure concentrations in AirToxScreen adjust the modeled ambient concentrations using the USEPA HAP Exposure Model [HAPEM (67)]. HAPEM accounts for exposure differences related to mobility patterns and indoor-outdoor differences in pollutant concentrations. *SI Appendix, Fig. S9* illustrates the ratio between AirToxScreen's ambient concentration and exposure concentration for all tracts in which we performed measurements for all HAPs that we measured. Ambient concentrations are typically higher (range of median values is 1 to 1.2 \times), though not in all cases, than the HAPEM-adjusted exposure concentration, which means AirToxScreen risk estimates are lower (by $\sim 20\%$) than they would be if ambient concentrations were used in place of exposure concentrations for calculating risk. This likely reflects the fact that residents in these tracts may not work near home, and likely commute to a place with lower ambient concentrations of these primary pollutants. We choose not to apply the HAPEM adjustment to our tract-level ambient concentration estimates. This difference of up to $\sim 20\%$ in calculated risk from AirToxScreen's choice of using exposure vs. ambient concentrations is relatively trivial compared to

the much-larger differences comparing to our measured estimates for all tracts but one.

Auxiliary Data Sources and Analysis.

Toxics release inventory. The TRI is a USEPA database used for tracking waste management of toxic chemicals, including air releases of HAPs (3). Reporting to TRI is mandatory for certain industry sectors, including oil refining, petrochemical manufacturing, and others relevant to the BR-NO corridor. We use TRI information to understand the spatial distribution of emissions sources of different chemicals and the magnitudes of their emissions, though, importantly, TRI-listed emissions are self-reported by industrial facilities (68). We downloaded TRI information using the online "TRI explorer" tool (https://enviro.epa.gov/triexplorer/tri_release.chemical?). These data were used to assess e.g., facility density across the state of Louisiana, the fraction of chloroprene emitted within our domain compared to the rest of the United States, and the number of ethylene oxide-emitting facilities along our driving route.

Air toxics screening assessment. AirToxScreen consists of modeled concentrations at the census tract level for 181 individual substances (16). It uses those modeled concentrations as the basis for cancer risk assessment and noncancer hazard assessment for a subset of compounds for which there are sufficient health data to estimate these effects. AirToxScreen employs dispersion modeling with coupled atmospheric chemistry modeling using emissions databases (e.g., NEI, TRI) of air toxics sources. Tract-level, ambient concentrations in AirToxScreen are areal averages of finer-scale estimates that reflect the annual average. We downloaded the most recent AirToxScreen ambient concentrations and cancer risk data (Year 2020, <https://www.epa.gov/AirToxScreen>) for comparison against our measurement. These data form the basis of Fig. 1 and those used to compare against risk estimates from measured air concentrations in Figs. 2A and 3. We include all of the AirToxScreen HAPs estimates in our comparisons with our own measurements, which comprise only a subset of those HAPs measured in AirToxScreen. We also downloaded data from previous AirToxScreen (and NATA) assessments to look at trends over time (*SI Appendix, Fig. S7*).

Formaldehyde seasonal correction. Atmospheric formaldehyde is both emitted directly and generated photochemically. Direct emissions include both anthropogenic (e.g., vehicles) and biogenic sources (e.g., vegetation, biomass burning) (42). Secondary formaldehyde is generated from the oxidation of both anthropogenic (e.g., ethene) and biogenic (e.g., isoprene) precursors (69). On regional scales, there is substantial spatial variability in the fraction of primary vs. secondary formaldehyde (70, 71) and formaldehyde concentrations (72), generally. According to statewide estimates for Louisiana in 2020 AirToxScreen, the large majority of formaldehyde is attributed either to secondary generation ($\sim 77\%$; see *SI Appendix, Fig. S3A*) or biogenic direct emissions ($\sim 20\%$), both of which are subject to seasonal variation (73, 74) driven by solar flux and underlying emissions.

Because our formaldehyde measurements were conducted in February, they almost certainly do not reflect an annual average. We adjusted our measured formaldehyde concentrations using a "seasonal correction factor." Using data from a variety of USEPA monitoring sites in the southeastern United States that measure formaldehyde, we calculated "percentage of annual average" values for all monitors across all months, shown in *SI Appendix, Fig. S3B*. The median for February is 63% of the annual average, and so we multiplied all of our aggregated formaldehyde concentrations by this seasonal correction factor of 1.58 (one divided by 0.63) in order to better reflect annual average values and compare with those in AirToxScreen.

Data, Materials, and Software Availability. Hazardous air pollutant (HAP) concentrations data have been deposited in Louisiana HAP-MAP Project (<https://doi.org/10.17605/OSF.IO/ABZYF>). Previously published data were used for this work (39).

ACKNOWLEDGMENTS. This project was made possible through financial support from Bloomberg Philanthropies (Grant ID 2021-100480). P.F.D., K.K., A.M.R., and S.N.L. also received financial support from the National Institute of Environmental Health Sciences (NIEHS, Grant ID P30ES032756). K.K. received additional financial support from NIEHS (Grant ID P2CES033415).

The development and commercialization of the Aerodyne Ethylene Oxide analyzer with 400 m cell was supported by the United States Environmental Protection Agency Small Business Innovation Research Program (Grant ID 68HERC21C0047); the United States Environmental Protection Agency has not reviewed this content and all conclusions are those of the authors alone. Local partners in southeastern Louisiana provided important guidance and connections that helped facilitate the project in many ways; these include: Louisiana Bucket Brigade, Inclusive Louisiana, Tulane Environmental Law Clinic, and RISE St. James. We also thank all operators of the Aerodyne Mobile Laboratory who worked on in-field sampling and data analysis for this phase of the Hazardous Air Pollutant Mapping and Assessment Project (HAP-MAP); these include: Kenji Lizardo, Ben Moul, Manjula Canagaratna, Harald Stark, Zach Payne, and Tim Onasch.

1. U.S. Energy Information Administration, Louisiana State Energy Profile (2024). <https://www.eia.gov/state/print.php?sid=LA>. Accessed 19 November 2024.
2. U.S. Department of Commerce, Made in America: Chemicals (2015). <https://www.commerce.gov/sites/default/files/migrated/reports/chemical-manufacturing-industry-profile.pdf>. Accessed 19 November 2024.
3. U.S. Environmental Protection Agency, Toxics Release Inventory (TRI) Program (2023). <https://www.epa.gov/toxics-release-inventory-tri-program>. Accessed 1 November 2023.
4. P. C. Pezzullo, Touring "Cancer Alley," Louisiana: Performances of community and memory for environmental justice. *Text Perform. Q.* **23**, 226–252 (2003).
5. Earthjustice, Cancer alley rises up (2024). <https://earthjustice.org/feature/cancer-alley-rises-up>. Accessed 1 November 2024.
6. I. Castellon, Cancer alley and the fight against environmental racism. *Villanova Environ. Law J.* **32**, 16–43 (2021).
7. K. A. Terrell, G. N. S. Julien, M. E. Wallace, Toxic air pollution and concentrated social deprivation are associated with low birthweight and preterm Birth in Louisiana *. *Environ. Res. Heal.* **2**, 021002 (2024).
8. L. Maniscalco *et al.*, "Cancer incidence in Louisiana by census tract: 2011–2020" (Tech. Rep., LSU Health, New Orleans, LA, 2024).
9. W. James, C. Jia, S. Kedia, Uneven magnitude of disparities in cancer risks from air toxics. *Int. J. Environ. Res. Public Health* **9**, 4365–4385 (2012).
10. K. A. Terrell, G. S. Julien, Air pollution is linked to higher cancer rates among black or impoverished communities in Louisiana. *Environ. Res. Lett.* **17**, 014033 (2022).
11. R. Nagra, R. Taylor, M. Hampton, L. Hilderbrand, "Waiting to Die": Toxic emissions and disease near the denka performance elastomer neoprene facility in Louisiana's cancer alley. *Environ. Just.* **14**, 14–32 (2021).
12. H. Parker, *EPA Investigation into Louisiana Agencies Yields Evidence of Racial Discrimination* (WWNO–New Orleans Public Radio, 2024).
13. K. A. Terrell, G. S. Julien, Discriminatory outcomes of industrial air permitting in Louisiana, United States. *Environ. Challenges* **10**, 100672 (2023).
14. J. Canicosa, *The Term "Cancer Alley" Has a Long History in Louisiana—And Even a History Before Louisiana* (Louisiana Illuminator, 2021).
15. U.S. Environmental Protection Agency, 2019 air toxics screening assessment (2022). <https://www.epa.gov/AirToxScreen/2019-airtoxscreen-assessment-results>. Accessed 1 November 2023.
16. U.S. Environmental Protection Agency, Technical support document for 2020 air toxics screening assessment (2024). https://www.epa.gov/system/files/documents/2024-05/airtoxscreen_2020-tds.pdf. Accessed 1 June 2024.
17. U.S. Environmental Protection Agency, National Emissions Inventory (NEI) (2023). <https://www.epa.gov/air-emissions-inventories/national-emissions-inventory-nei>. Accessed 1 June 2024.
18. B. Young *et al.*, A system for standardizing and combining U.S. Environmental Protection Agency emissions and waste inventory data. *Appl. Sci.* **12**, 3447 (2022).
19. E. Garcia *et al.*, Evaluation of the agreement between modeled and monitored ambient hazardous air pollutants in California. *Int. J. Environ. Res. Heal.* **24**, 363–377 (2014).
20. P. J. Lupo, E. Symanski, A comparative analysis of modeled and monitored ambient hazardous air pollutants in Texas: A novel approach using concordance correlation. *J. Air Waste Manage. Assoc.* **59**, 1278–1286 (2009).
21. J. M. Logue, M. J. Small, A. L. Robinson, Evaluating the national air toxics assessment (NATA): Comparison of predicted and measured air toxics concentrations, risks, and sources in Pittsburgh, Pennsylvania. *Atmos. Environ.* **45**, 476–484 (2011).
22. D. C. Payne-Sturges, T. A. Burke, P. Breyse, M. Diener-West, T. J. Buckley, Personal exposure meets risk assessment: A comparison of measured and modeled exposures and risks in an urban community. *Environ. Heal. Perspect.* **112**, 589–598 (2004).
23. B. J. George *et al.*, An evaluation of EPA's National-Scale Air Toxics Assessment (NATA): Comparison with benzene measurements in Detroit, Michigan. *Atmos. Environ.* **45**, 3301–3308 (2011).
24. M. W. Tehrani *et al.*, Characterizing metals in particulate pollution in communities at the fenceline of heavy industry: Combining mobile monitoring and size-resolved filter measurements. *Environ. Sci.: Process. Impacts* **25**, 1491–1504 (2023).
25. Z. Xue, C. Jia, A model-to-monitor evaluation of 2011 National-Scale Air Toxics Assessment (NATA). *Toxics* **7**, 13 (2019).
26. L. E. Padilla, D. R. Peters, E. J. Mohr, R. A. Alvarez, Ambient measurements of hazardous air pollutants in the United States routinely exceed predictions from screening-level exposure models. *Environ. Sci. Technol. Lett.* **12**, 57–63 (2025).
27. Louisiana Department of Environmental Quality, Ambient air monitoring data & reports (2024). <https://www.deq.louisiana.gov/page/ambient-air-monitoring-data-reports>. Accessed 1 November 2024.
28. L. Phelps, Compendium method to-15: Determination of volatile organic compounds (VOCs) in air collected in specially-prepared canisters and analyzed by gas chromatography/mass spectrometry (GC/MS). *U.S. Environmental Protection Agency* (2021). <https://www.epa.gov/sites/default/files/2021-05/documents/ord-eto-canister-background-memo-05072021.pdf>. Accessed 1 November 2023.

Author affiliations: ^aDepartment of Environmental Health and Engineering, Johns Hopkins University, Baltimore, MD 21205; ^bThe Risk Sciences and Public Policy Institute, Johns Hopkins University, Baltimore, MD 21205; ^cCenter for Aerosol and Cloud Chemistry, Aerodyne Research, Inc., Billerica, MA 01821; and ^dCenter for Atmospheric and Environmental Chemistry, Aerodyne Research, Inc., Billerica, MA 01821

Author contributions: E.S.R., M.S.C., T.I.Y., C.D., S.C.H., T.A.B., A.M.R., K.K., K.E.N., and P.F.D. designed research; E.S.R., A.Y., S.A., M.W.T., S.N.L., A.A.C., C.G., M.S.C., B.M.L., T.I.Y., J.R.R., S.C.H., A.M.A., C.D., E.M.L., E.C.F., B.S.W., A.M.R., K.K., K.E.N., and P.F.D. performed research; M.S.C. contributed new reagents/analytic tools; E.S.R., A.Y., M.S.C., T.I.Y., J.R.R., S.C.H., A.M.A., E.M.L., E.C.F., and B.S.W. analyzed data; and E.S.R. wrote the paper.

The authors declare no competing interest.

This article is a PNAS Direct Submission. J.D.M. is a guest editor invited by the Editorial Board.

Copyright © 2025 the Author(s). Published by PNAS. This open access article is distributed under [Creative Commons Attribution-NonCommercial-NoDerivatives License 4.0 \(CC BY-NC-ND\)](https://creativecommons.org/licenses/by-nc-nd/4.0/).

29. U.S. Environmental Protection Agency, Evaluation of the inhalation carcinogenicity of ethylene oxide (2016). https://iris.epa.gov/static/pdfs/1025_summary.pdf. Accessed 1 November 2024.
30. U.S. Environmental Protection Agency, Chloroprene assessment summary (2020). https://iris.epa.gov/static/pdfs/1021_summary.pdf. Accessed 1 November 2024.
31. U.S. Environmental Protection Agency, IRIS toxicological review of formaldehyde (inhalation) (2024). https://iris.epa.gov/static/pdfs/0419_summary.pdf. Accessed 1 November 2024.
32. J. S. Apte, C. Manchanda, High-resolution urban air pollution mapping. *Science* **385**, 380–385 (2024).
33. J. Kerckhoffs *et al.*, Mobile monitoring of air pollution—A position paper on use cases, good practices, challenges, and opportunities. *Environ. Int.* **202**, 109582 (2025).
34. J. S. Apte *et al.*, High-resolution air pollution mapping with Google Street view cars: Exploiting big data. *Environ. Sci. Technol.* **51**, 6999–7008 (2017).
35. D. J. Miller *et al.*, Characterizing elevated urban air pollutant spatial patterns with mobile monitoring in Houston, Texas. *Environ. Sci. Technol.* **54**, 2133–2142 (2020).
36. P. Gu *et al.*, Intracity variability of particulate matter exposure is driven by carbonaceous sources and correlated with land-use variables. *Environ. Sci. Technol.* **52**, 11545–11554 (2018).
37. T. I. Yacovitch *et al.*, Mobile laboratory investigations of industrial point source emissions during the MOOSE field campaign. *Atmosphere* **14**, 1632 (2023).
38. E. Galarneau *et al.*, From hotspots to background: High-resolution mapping of ethylene oxide in urban air. *Atmos. Environ.* **307**, 119828 (2023).
39. E. S. Robinson *et al.*, Ethylene oxide in Southeastern Louisiana's petrochemical corridor: High spatial resolution mobile monitoring during HAP-MAP. *Environ. Sci. Technol.* **58**, 11084–11095 (2024).
40. U.S. Environmental Protection Agency, Integrated risk information system (2024). <https://www.epa.gov/iris>. Accessed 1 November 2024.
41. D. Clay, Memorandum: Role of the baseline risk assessment in superfund remedy selection decisions. *U.S. Environmental Protection Agency* (1991). <https://www.epa.gov/sites/default/files/2015-11/documents/baseline.pdf>. Accessed 1 November 2023.
42. U.S. Environmental Protection Agency, Locating and estimating air emissions from sources of formaldehyde (revised) (1991). <https://www.epa.gov/sites/default/files/2020-11/documents/formaldehyde.pdf>. Accessed 1 November 2024.
43. J. Brydson, *Plastics Materials (Seventh Edition)* (Elsevier, 1995).
44. U.S. Environmental Protection Agency, Benzidine assessment summary (1989). https://iris.epa.gov/static/pdfs/0135_summary.pdf. Accessed 1 November 2024.
45. U.S. Environmental Protection Agency, LaPlace, St. John the Baptist Parish, Louisiana (2024). <https://www.epa.gov/la/laplace-st-john-baptist-parish-louisiana>. Accessed 1 November 2024.
46. T. L. B. Yelverton, M. D. Hays, J. Rice, Ethylene oxide: An air contaminant of concern. *ACS ES&T Air* **1**, 747–754 (2024).
47. I. George, H. Vreeland, J. Faircloth, P. Kariher, W. Preston, Optimized approach for measuring ethylene oxide in mobile source exhaust. *Environ. Sci. Technol. Lett.* **11**, 560–565 (2024).
48. J. Hoisington, J. S. Herrington, Rapid determination of ethylene oxide and 75 VOCs in ambient air with canister sampling and associated growth issues. *Separations* **8**, 35 (2021).
49. S. Spooner *et al.*, A comparison of ambient air ethylene oxide modeling estimates from facility stack and fugitive emissions to canister-based ambient air measurements in Salt Lake City. *Air* **1**, 175–183 (2023).
50. T. I. Yacovitch *et al.*, Ethylene oxide monitor with part-per-trillion precision for in situ measurements. *Atmos. Meas. Tech.* **16**, 1915–1921 (2023).
51. U.S. Health and Human Services, Evaluation of ethylene oxide concentrations in outdoor air near sterigenics (EPA facility ID: IL0000433594, Willowbrook, Dupage County, IL, 2023). <https://www.atsdr.cdc.gov/HAC/pha/sterigenics/Sterigenics-HC-Public-Comment-508.pdf>. Accessed 1 November 2024.
52. U.S. Environmental Protection Agency, Air toxics screening assessment (2020). <https://www.epa.gov/AirToxScreen/2020-airtoxscreen-assessment-results>. Accessed 1 June 2024.
53. IARC Working Group on the Evaluation of Carcinogenic Risks to Humans, "Some aromatic amines, organic dyes, and related exposures" (Tech. Rep., International Agency for Research on Cancer, 2010).
54. U.S. Environmental Protection Agency, Acrylonitrile assessment summary (1987). https://iris.epa.gov/static/pdfs/0206_summary.pdf. Accessed 22 April 2025.
55. S. C. Herndon *et al.*, Characterization of urban pollutant emission fluxes and ambient concentration distributions using a mobile laboratory with rapid response instrumentation. *Faraday Discuss.* **130**, 327–339 (2005).
56. T. I. Yacovitch *et al.*, Air pollutant mapping with a mobile laboratory during the BEE-TEX field study. *Environ. Heal. Insights* **9**, 7–13 (2015).
57. A. C. Targino, M. V. B. Oliveira, P. Krecel, Ubiquity of hazardous airborne substances on passenger ferries. *J. Hazard. Mater.* **423**, 127133 (2022).
58. E. S. Robinson *et al.*, Wintertime spatial patterns of particulate matter in Fairbanks, AK during ALPACA2022. *Environ. Sci. Atmos.* **3**, 568–580 (2023).
59. R. Jimenez *et al.*, "Atmospheric trace gas measurements using a dual quantum-cascade laser mid-infrared absorption spectrometer" in *Novel In-Plane Semiconductor Lasers IV* (2005), pp. 318–331.

60. E. Spinei *et al.*, The first evaluation of formaldehyde column observations by improved Pandora spectrometers during the KORUS-AQ field study. *Atmos. Meas. Tech.* **11**, 4943–4961 (2018).
61. I. Gordon *et al.*, The HITRAN2020 molecular spectroscopic database. *J. Quant. Spectrosc. Radiat. Transf.* **277**, 107949 (2022).
62. M. S. Clafin *et al.*, An in situ gas chromatograph with automatic detector switching between PTR and EI-TOF-MS: Isomer-resolved measurements of indoor air. *Atmos. Meas. Tech.* **14**, 133–152 (2020).
63. R. W. Hornung, L. D. Reed, Estimation of average concentration in the presence of nondetectable values. *Appl. Occup. Environ. Hyg.* **5**, 46–51 (1990).
64. E. Pebesma, Simple features for R: Standardized support for spatial vector data. *R.J.* **10**, 439 (2018).
65. D. Kahle, H. Wickham, ggmap: Spatial Visualization with ggplot2. *R.J.* **5**, 144 (2013).
66. H. A. Barton *et al.*, Assessing susceptibility from early-life exposure to carcinogens. *Environ. Heal. Perspect.* **113**, 1125–1133 (2005).
67. U.S. Environmental Protection Agency, Human exposure modeling—Hazardous air pollutant exposure model (HAPEM) (2015). <https://www.epa.gov/fera/human-exposure-modeling-hazardous-air-pollutant-exposure-model-hapem>. Accessed 1 November 2024.
68. U.S. Environmental Protection Agency, Reporting for TRI facilities (2024). <https://www.epa.gov/toxics-release-inventory-tri-program/reporting-tri-facilities>. Accessed 1 November 2024.
69. R. Atkinson, J. Arey, Gas-phase tropospheric chemistry of biogenic volatile organic compounds: A review. *Atmos. Environ.* **37**, 197–219 (2003).
70. L. A. J. Bastien, N. J. Brown, R. A. Harley, Contributions to local- and regional-scale formaldehyde concentrations. *Atmos. Chem. Phys.* **19**, 8363–8381 (2019).
71. D. Luecken, W. Hutzell, M. Strum, G. Pouliot, Regional sources of atmospheric formaldehyde and acetaldehyde, and implications for atmospheric modeling. *Atmos. Environ.* **47**, 477–490 (2012).
72. I. D. Smedt *et al.*, Comparative assessment of TROPOMI and OMI formaldehyde observations and validation against MAX-DOAS network column measurements. *Atmos. Chem. Phys.* **21**, 12561–12593 (2021).
73. M. Bauwens *et al.*, Nine years of global hydrocarbon emissions based on source inversion of OMI formaldehyde observations. *Atmos. Chem. Phys.* **16**, 10133–10158 (2016).
74. C. Shim *et al.*, Constraining global isoprene emissions with Global Ozone Monitoring Experiment (GOME) formaldehyde column measurements. *J. Geophys. Res. Atmos.* **110**, D24301 (2005).